Old Dominion University
ODU Digital Commons

Bioelectrics Publications | Frank Reidy Research Center for Bioelectrics

2002

Electrical Network-Based Time-Dependent Model of Electrical Breakdown in Water

R. P. Joshi
Old Dominion University

J. Qian
Old Dominion University

K. H. Schoenbach
Old Dominion University

Follow this and additional works at: https://digitalcommons.odu.edu/bioelectrics_pubs

Part of the Electrical and Electronics Commons, and the Radiochemistry Commons

Repository Citation

Joshi, R. P.; Qian, J.; and Schoenbach, K. H., "Electrical Network-Based Time-Dependent Model of Electrical Breakdown in Water" (2002). *Bioelectrics Publications*. 244.
https://digitalcommons.odu.edu/bioelectrics_pubs/244

Original Publication Citation

Joshi, R. P., Qian, J., & Schoenbach, K. H. (2002). Electrical network-based time-dependent model of electrical breakdown in water. *Journal of Applied Physics, 92*(10), 6245-6251. doi:10.1063/1.1515105

This Article is brought to you for free and open access by the Frank Reidy Research Center for Bioelectrics at ODU Digital Commons. It has been accepted for inclusion in Bioelectrics Publications by an authorized administrator of ODU Digital Commons. For more information, please contact digitalcommons@odu.edu.

Electrical network-based time-dependent model of electrical breakdown in water

R. P. Joshi,[a] J. Qian, and K. H. Schoenbach
Department of Electrical and Computer Engineering, Old Dominion University, Norfolk, Virginia 23529-0246

(Received 15 July 2002; accepted 23 August 2002)

A time-dependent, two-dimensional, percolative approach to model dielectric breakdown based on a network of parallel resistor–capacitor elements having random values, has been developed. The breakdown criteria rely on a threshold electric field and on energy dissipation exceeding the heat of vaporization. By carrying out this time-dependent analysis, the development and propagation of streamers and prebreakdown dynamical evolution have been obtained directly. These model simulations also provide the streamer shape, characteristics such as streamer velocity, the prebreakdown delay time, time-dependent current, and relationship between breakdown times, and applied electric fields for a given geometry. The results agree well with experimental data and reports in literature. The time to breakdown (t_{br}) for a 100 μm water gap has been shown to be strong function of the applied bias, with a 15–185 ns range. It is also shown that the current is fashioned not only by dynamic changes in local resistance, but that capacitive modifications arising from vaporization and streamer development also affect the transient behavior. © *2002 American Institute of Physics.* [DOI: 10.1063/1.1515105]

I. INTRODUCTION

There is considerable interest in the study of electrical breakdown in water (and other liquids) for a variety of reasons.[1] Practical applications of dielectric liquids include water-filled gaps for the design of acoustic equipment,[2,3] the insulation of high-voltage devices,[4] as the medium in spark erosion machines,[5] and use in energy storage and switching elements for pulsed power systems. From a dielectrics breakdown standpoint, liquids seem to have some advantages over gas systems, as their electric breakdown strengths are higher. In comparison to solids, their ability to circulate leads to better thermal management and homogeneity. Liquid dielectrics are also better suited for applications involving complex geometries.

Dielectric breakdown in liquids, gases, and solid insulators is frequently characterized by two features: (1) the occurrence of narrow discharge channels, and (ii) a strong tendency of these channels to branch into complicated stochastic patterns. Typical examples include lightning,[6] surface discharges leading to Lichtenberg figures,[7] and treeing in polymers.[8] The mechanisms responsible for the breakdown in dielectric liquids have long been the subject of many speculations, and two principle theories have emerged: (i) a bubble initiated breakdown process, and (ii) an electronic process. The observed influence of hydrostatic pressure on the breakdown strength, the results of chromatographic analyses, and application of optical techniques, have helped clarify the physics.[9,10] It is now accepted that liquid electrical breakdown proceeds through the creation and propagation of streamers over regions of low density.[11–15] Spectroscopic analyses of light emitted by streamers indicate, that in the presence of small concentrations of electronic scavenger additives, electronic processes can also be present.[16] The propagation of streamers in water breakdown is explained as the evaporation of water at the tip of the streamer and the region around it.[17] Thus, streamers are essentially gas discharges in thin vapor bubbles. The rationale for thermal processes playing a decisive role in water breakdown is based on the fact that electron avalanche processes in liquids are nearly negligible.[18] This is because the electric fields necessary to impart electrons with energy large enough to impact ionization, exceed the observed breakdown values. Also, free electrons are generally absent in water since an enormous increase in entropy is required to convert an electron into a negative ion by attachment. This dearth of free electrons can alternatively be viewed as arising from the large ''band gap'' of water, which is ~6.9 eV.[19] Finally, the observed dependence of breakdown on hydrostatic pressure and voltage pulse duration point toward the importance of the vapor bubble formation process. For example, a high hydrostatic pressure inhibits bubble formation resulting in an observed increase of the hold-off strength.[20] Similarly, longer pulses allow more time for bubble nucleation, and thereby, are seen to decrease the breakdown field requirements.

Several analytical models and simulation studies of streamers in liquid and gas dielectrics have probed the streamer initiation and propagation processes.[21–26] Most have been based on deterministic and continuum methods. Only a few stochastic approaches have been reported to account for the random internal fluctuations, and successfully predicted the ''treelike'' branching behavior.[27–29] Such random models, however, are not unique to this field of study, and have also been applied to treat transport in sintered composites with grain boundaries,[30] or for quenched random media.[31] Despite these advances in modeling and use of so-

[a]Electronic mail: rjoshi@odu.edu

 © 2002 American Institute of Physics

phisticated simulation approaches, a comprehensive treatment that combines the temporal evolution, a multidimensional spatial aspect and inclusion of the internal randomness has still not been well developed. The only report, to the best of our knowledge, has been by Beroual's group in France recently.[32]

In this contribution, a percolative approach to modeling dielectric breakdown is presented. Conduction is treated in terms of current flows through a network of parallel resistor–capacitor elements having random values (very small deviations based on a Gaussian distribution with fixed mean). The method relies on carrying out self-consistent evaluations of the local potentials based on Kirchhoff circuit analysis at each time step starting from a given initial condition. The current flows through each elemental unit and local heat dissipation can be determined. A set of two breakdown criteria, a threshold electric field and energy dissipation greater than the heat of vaporization, are used to ascertain the electrical breakdown of a given element. By carrying out this time-dependent analysis of a two-dimensional (2D) electrical network, the development and propagation of streamers and prebreakdown dynamical evolution can be obtained directly. Breakdown of the overall structure occurs if a ''failure channel'' percolates all the way from one electrode to the other. This model simulation also provides streamer shape and characteristics such as streamer velocity, the prebreakdown delay time, and the relationship between breakdown times and applied electric field for a given geometry. The results agree well with experimental data and reports in literature.

II. SIMULATION DETAILS

The simulation model is developed and implemented by considering a 2D regular network in which the two sides (left- and right-hand side) represent the electrodes. A 2D representation has been used for simplicity, but the approach can easily be extended for three-dimensional analysis as well. Each unit of this electrical network consists of a parallel resistor–capacitor combination whose attributes are based on the geometry and local parameters. The values can either be uniformly constant or assigned a random variation to account for local fluctuations. Variations can arise from the presence of bubbles, variable solute concentrations and fractional compositions in the case of mixtures. The use of Gaussian distribution function with user specified mean values $\langle R\rangle$ and $\langle C\rangle$, and variances σ_R, σ_C can provide for randomness.

Here, a point-plane electrode geometry, that is commonly used in experimental work, has been chosen for concreteness. Such an arrangement can create a large, localized electric field at the tip for initiating the breakdown. This geometric arrangement can be modeled by dividing the region into $n\times m$ elements as shown in Fig. 1. The narrow rectangles on the two sides of the model donate the positive and negative electrodes. Every line segment of the network shown in Fig. 1 donates a single electrical elemental unit consisting of a parallel resistor–capacitor combination as shown in Fig. 2. The total number of electrical units, N_T, in such a $n\times m$ network is: $N_T=4\times m\times n$. Assuming each element as a cubic unit of conductivity σ, length L and area S,

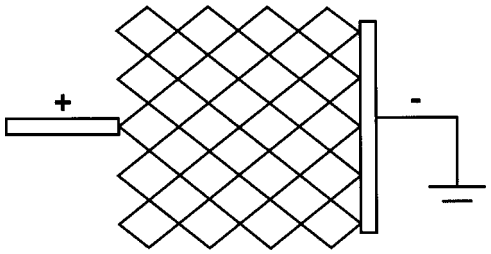

FIG. 1. A 4×5 network representation for a point-plane geometry.

its resistance R per unit will be: $R=L/[\sigma S]$. This resistance R can vary in sections, and thus, be dissimilar for the various elements. A Gaussian distribution with mean value $\langle R\rangle = L/[\sigma S]$ and standard variation $\delta_R=c\langle R\rangle$, with $0\leqslant c<1$, has been used here. The voltage assigned to each node is the unknown variable that can be obtained by solving the entire electrical network based on Kirchhoff's law.

In the present case, two parallel criteria have been used for the water breakdown. Both are general, and can be applied to any liquid dielectric. The first criteria for breakdown is that the electric (E) field across the electrical element be higher than a threshold value $E_{\text{threshold}}$ (i.e., $E_{\text{element}} > E_{\text{threshold}}$). This E field across each element can be computed since the simulation procedure continually provides the node voltages at each time step by simultaneously solving Kirchhoff equations (KCE). A second criteria is that the energy supplied by the local electrical element W_{sup} be higher than the latent heat W_{lat} of vaporization for the liquid. This condition is expressed as: $W_{\text{sup}}=[U^2_{\text{element}}/R_{\text{element}}]\Delta t$, where U_{element} is the voltage drop across the element and Δt the simulation time step. The latent power W_{lat} necessary to vaporize the water can be obtained directly from the equation:[33]

$$W_{\text{lat}}=\rho_0 V[c(T_2-T_1)+r], \tag{1}$$

with $\rho_0=998\ \text{kg m}^{-3}$, $c=4.18\times10^3\ \text{J kg}^{-1}, K^{-1}$, $T_2=373\ \text{K}$, $T_1=293\ \text{K}$, and $r=2256\ \text{kJ kg}^{-1}$. Thus, a thermal aspect is inherently included in the breakdown analyses. This has been done here because localized internal heating is known to produce expansion and bubble formation that results in density fluctuations. Increases in local temperature can also act to expand pre-existing bubbles by augmenting their internal pressure. As recently proposed, the resulting reductions in density over localized regions can trigger enhanced electron impact ionization.[20] In effect, the rarefied zones can, in principle, act as seed sites for triggering breakdown. In the present approach, solution of the KCE, yield both the current distribution in each branch of the network

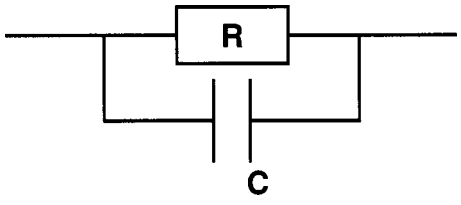

FIG. 2. The elemental unit representing the network in Fig. 1.

and the node voltages. Power dissipation density with each segment can thus be computed from their product. If at any time step, an elemental segment meets both the aforementioned criteria for breakdown, then that corresponding element is set to a ''breakdown state''.

In the present model, the following procedure has been implemented for determining the breakdown voltage ($V_{\rm br}$) for a network of given size. Since the breakdown voltage is not known *a priori*, a relatively low trial voltage is used as the external bias to start the calculations. The resistor and capacitor values are initialized with a Gaussian distribution. The internal node voltages and branch currents are then computed by solving the KCE. If the local electrical field exceeds the critical threshold and the energy dissipation is above the latent heat of vaporization, the elemental resistor and capacitor values change due to a breakdown event. The following simple, nonlinear current–voltage (I–V) relationship has been chosen:

$$R(E)=R_{oi}, \qquad \text{for } E<E_{\rm threshold}, \tag{2a}$$

$$\text{and } R(E)=R_{of}, \quad \text{for } E\geqslant E_{\rm threshold}, \tag{2b}$$

where E is the local electric field within each resistor segment, R_{oi} the initial random value assigned to the ith resistive segment based on the Gaussian distribution, and $R_{\rm of}$ the final value upon breakdown. Physically, in this simple nonlinear model, the resistance drops dramatically upon breakdown from R_{oi} to R_{of}. Here, the magnitude of R_{of} has been chosen to be at least 10^{-3} of the initial value. Thus, a relatively simple I–V nonlinearity was implemented to model a transition between a high resistance ''current blocking'' state to a low resistance ''conducting'' after breakdown. In principle, though, other more complicated nonlinear I–V characteristics[34–39] could easily be implemented. The overall calculation would proceed as outlined here, but the computational time for solving the set of coupled KCE would increase with complexity in the I–V characteristics. In addition, elemental breakdown results in an alteration of the capacitance value. Physically, this is necessary since the vaporization-based streamer development causes the local dielectric constant to decrease from the liquid value.

Using the updated impedance network at each time step (with or without elemental breakdown), a Kirchhoff solution is recomputed. The procedure repeats until a percolative path is established between the two electrodes, or no further transitions in the elemental impedances occur with time anywhere for the applied bias. The value of the applied voltage sets $V_{\rm br}$ in the former case. In the latter situation, with an absence of a complete percolation channel, the biasing voltage is increased, and the aforementioned procedure is repeated until an eventual a complete percolative path is achieved. It must be mentioned that the $V_{\rm br}$ value thus obtained for a given network array is not unique due to the fluctuations in initial random selected R_{oi} value set. Repeating the full procedure numerous times, the different random-number seeds, eliminates the statistical variation.

This procedure can thus yield the following quantities: (i) breakdown voltage for a given geometry and liquid dielectric parameter set, (ii) time to breakdown (i.e., the temporal delay of failure), (iii) streamer pattern (i.e., bushlike or filamentary) and its evolution in time, and (iv) the velocity of streamer propagation by accounting for the speed with which elemental units of the network break down in succession. The technique is thus fairly general and robust. It must be mentioned that it differs from a previous report of network-based analysis[32] because a deterministic circuit configuration graph is utilized here. Consequently, the spatially dependent electric fields and their values at the streamer heads can be calculated exactly. Furthermore, aspects such as contact curvatures and contact geometries (e.g., point versus planar) can also be taken into account. In the work by Aka-Ngnui and Beroual,[32] for example, such electric fields were estimated by invoking approximations. It might also be mentioned that due to the presence of a chosen electrical network, the streamer propagation in the present approach proceeds along predetermined segments, and does not have completely random orientation.

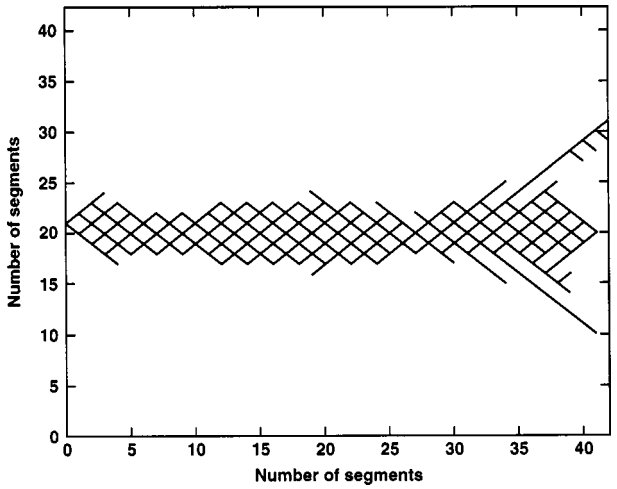

FIG. 3. Numerical results of a breakdown percolative path a 40×40 network with $\sigma_R=250$ ohms. A filamentary-type structure is predicted.

III. RESULTS AND DISCUSSION

Simulations for breakdown in a dielectric (such as purified/deionized water which is of interest to the pulsed-power community) were carried out based on the procedure outlined in Sec. II. The value of $E_{\rm threshold}$ was set to 6×10^{7} V m^{-1} in keeping with experimental reports on breakdown in water.[20,40] A small σ_R of 50 ohms was taken to mimic the internal nonuniformities in conductance. These values were chosen to match the available experimental data, as discussed later. For simplicity, the results obtained here were for $n=m$. Simulation results showing the final breakdown condition for a 40×40 network with an applied voltage of 7 kV are provided in Fig. 3. A filamentary-type breakdown structure with a complete percolative path is obvious. The total physical dimensions for the network along each direction were taken to be 10^{-4} m. Thus, under ideal conditions (i.e., identical segments), a breakdown voltage of 6 kV is expected. In the presence of internal inhomogeneities and the sharp anode geometry, one expects the overall breakdown voltage to be lower. Here, however, a much higher applied

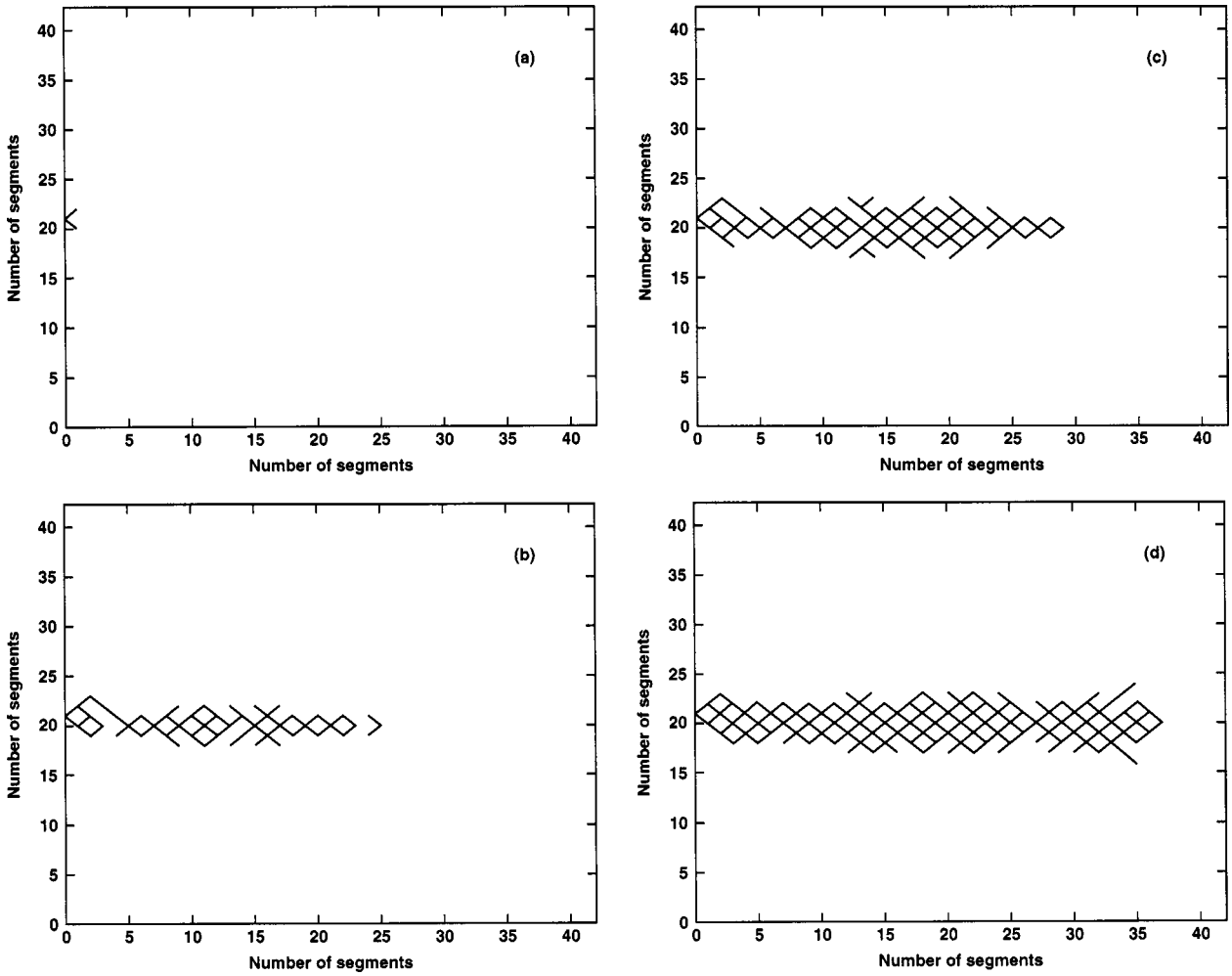

FIG. 4. Simulation result showing the breakdown structure for the network of Fig. 3 during the transient phase at time instants of: (a) 0.1356 μ, (b) 0.1587 μs, (c) 1.655 μs, and (d) 1.723 μs. Propagation and incomplete percolation are obvious.

voltage of 7 kV was taken to ensure breakdown would occur and that the duration would not be excessively large. The total time taken to achieve this final breakdown state was 1.85×10^{-7} s. This simulation demonstrates that breakdown involves the development of filamentary branches with associated random structure, followed by a complete percolative path. This is in keeping with experimental observations. Due to the slight variation σ_R in the initial resistor assignment, the breakdown is not completely symmetric.

Simulation result of the breakdown structure during the transient phase, for the network of Fig. 3 at different time instants is shown in Figs. 4(a)–4(d). The times were 0.1356 μs, 0.1587 μs, 1.655 μs, and 1.723 μs, respectively. Propagating breakdown segments and progressive percolation are obvious. Also, the breakdown is predicted to initiate at the left-hand side electrode because of the higher electric field associated with the sharper geometry. Given the temporal nature of the present simulations, it was possible to compute the time to breakdown for a range of electric fields. The breakdown delay times thus obtained are plotted in Fig. 5 as a function of the applied field. Experimental data on water breakdown obtained in our laboratory are also shown for comparison. The experimental data were obtained by using pulsed voltages and the test circuit shown schematically in Fig. 6. The test switch had a compact size and allowed its integration into a two-stage pulse generator system. The gap spacing between the electrodes could be adjusted to an accuracy of 10 μm. A water outlet and an inlet were also included

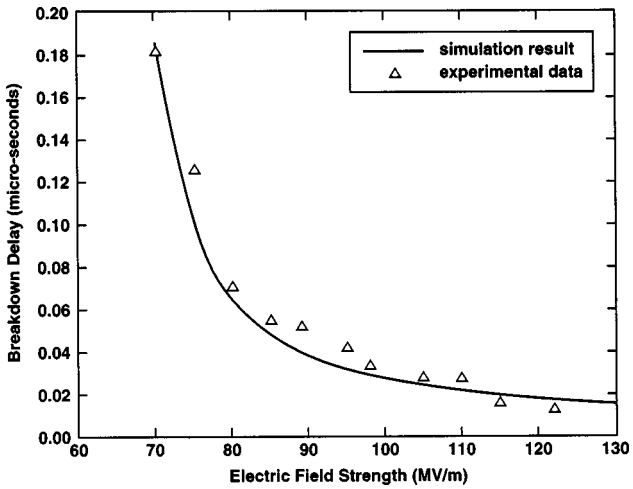

FIG. 5. Plot of simulated breakdown delay times vs the applied electric field strength for water in a 100 μm electrode gap. Available experimental data are also shown and reveal good quantitative agreement.

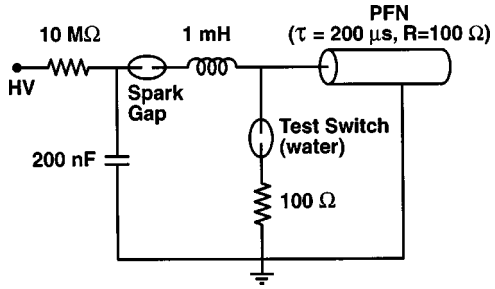

FIG. 6. Schematic of the water switch and electrical circuit used in experiments.

to enable operation under ''flow'' conditions. The stored energy was in a 200 nF charging capacitor, which could be discharged via a primary switch triggered through a transistor-transistor logic (TTL) signal. The second-stage energy store was in a 5 ns, 100 Ω, and 93 mm length of a serpentine stripline having a total capacitance of 100 pF. The stripline was resonantly charged through a large choking inductance so as to reduce the charging current and protect the semiconductor switch. During the charging phase, the test switch acts as a simple load.

The plot of Fig. 5 for breakdown times versus applied electric field, were for a 100 μm electrode gap. A comparison between the available experimental data and simulation results reveal very good quantitative agreement. The durations of the prebreakdown phase ranged from 15 to about 185 ns. A threshold electric field (E_{br}) for breakdown is evident, and for values close to E_{br}, inordinately long times are predicted for total failure. This trend is in keeping with the universal trends in breakdown durations of dielectrics under electric stress. Based on the time-dependent percolative model developed here, it becomes possible to monitor the successive movement of the elemental units as they break down sequentially. This, in essence, yields the propagation speed of the streamer tip as a function of time. Calculation results for the temporal development of the streamer speed are plotted in Fig. 7 for an applied voltage of 7 kV. The plot shows that a finite nonzero time duration is required for the

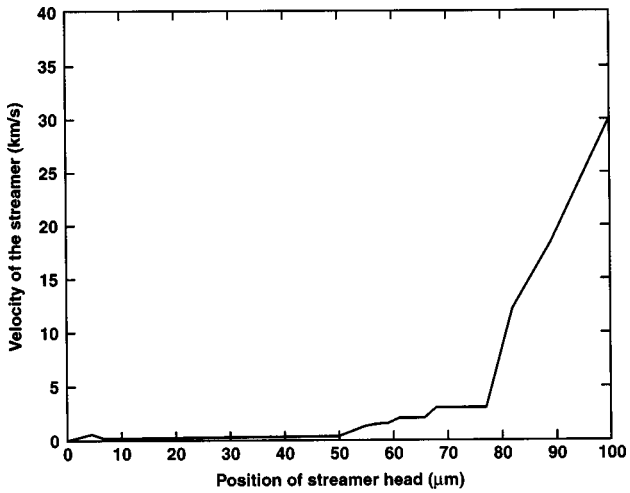

FIG. 7. Calculated streamer velocity under a 7 kV external electric field condition for the 100 μm electrode gap.

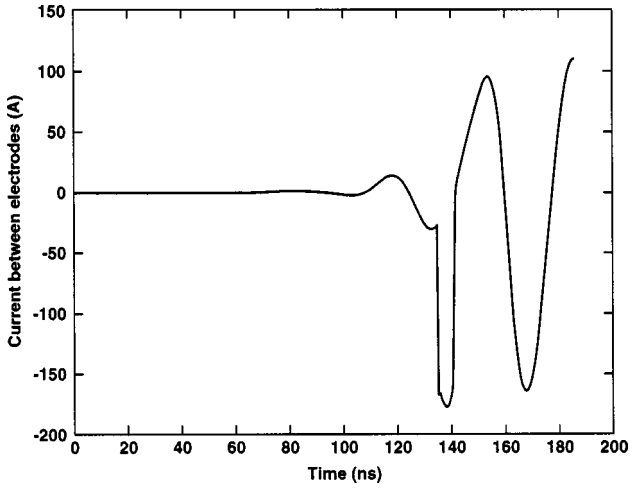

FIG. 8. Calculated circuit current as a function of time prior to and immediately following liquid breakdown.

streamer to form. Hence, initially, the streamer velocity is zero, and remains small as the streamer tip slowly advances toward the opposite side. Once the streamer has reached about 50% of the anode–cathode distance, the velocity begins to increase. Toward the end of this process, the velocity is predicted to reach high values in the 10^4–3×10^4 ms^{-1} range, with a peak just prior to the completion of a percolative path. The streamer speeds obtained here compare very well with the experimental report of a 1.2×10^4 ms^{-1} average value by Lisitsyn *et al.*[17] The existence of a slow initial phase, followed by more rapid streamer propagation as obtained in the simulations here, has also been reported.[24] More importantly, the temporal development of streamer velocity matches Akiyama's experimental data on water breakdown.[1] The measured values were roughly 2×10^2 ms^{-1} during the initial initiation phase. This was followed by streamer velocities around 4×10^3 ms^{-1}, with final speeds of 4×10^4 ms^{-1}.[1]

Finally, simulation results for the temporal development of current in water, are shown in Fig. 8. Prior to breakdown, the current is negligible, but stable. Transient behavior is seen to appear at around 1.15×10^{-7} s. The following features of the prebreakdown phase are evident from Fig. 8. (i) first, fluctuations in current appear beyond 1.15×10^{-7} s that are accompanied by large swings in magnitude. *Both positive and negative values are predicted.* Such multiple reversals in the current flow direction, have been reported in recent experiments by our group.[41] Hence, the predicted current excursions of Fig. 8, into both the positive and negative domain, are in agreement with measured data, (ii) the absolute magnitudes of the peak currents in Fig. 8, are seen to be around 150 A. These values match reported experimental data[41] very well. Hence, a rough quantitative concurrence is also seen to emerge, and (iii) despite the multiple excursions into the negative domain, the current eventually tends to approach a relatively large positive value. This implies that eventually, as the final breakdown state approaches, the system settles down into a low resistance stable mode. This breakdown state, as already indicated in Fig. 3, is filamentary in nature.

Direction reversal of circuit current and the occurrence of negative values in Fig. 8 during the breakdown phase is of interest, and deserves some discussion. Though the details are complex and fashioned collective by the time-dependent behavior of all the resistor–capacitor elements, a simple physical understanding is provided, by considering the breakdown of a single unit as shown in Fig. 2. The total current $I(t)$ across the resistor–capacitor combination of Fig. 2 is given as:

$$I(t)=d[C(t)*V(t)]/dt+V(t)/R(t), \tag{3}$$

where the capacitance $C(t)$, the resistance $R(t)$, and elemental voltage drop $V(t)$ can all be time dependent. Physically, as the breakdown process starts, the elemental resistance is expected to reduce for two reasons. First, the localized vaporization leads to a creation (or growth) of a low-density region, in which scattering and inelastic scattering losses are lowered. This would effectively enhance the mobility and local electrical conductance. Second, the impact ionization and electron initiated generation would increase within the localized region, also leading to a decrease in the resistance $R(t)$. Hence, the final resistance R_f following breakdown would be less than the R_{ini} value prior to the breakdown process. A capacitive change would also be associated with localized vaporization, or bubble formation or increase in a low-density localized region. This would arise since the relative dielectric constant would change from about 81 (the value for water), to a low value near unity (the value for air/gas). The exact value though, would be dependent on the physical dimensions of the rarefied zone. In any case, the final value C_f in the breakdown state would be less than the prebreakdown value of C_{ini} (i.e., $C_f<C_{\text{ini}}$.) Letting the following simple temporal relation model the time evolution of $R(t)$ and $C(t)$:

$$R(t)=[R_{\text{ini}}-R_f]*\exp[-K_1*t]+R_f, \tag{4a}$$

and

$$C(t)=[C_{\text{ini}}-C_f]*\exp[-K_2*t]+C_f, \tag{4b}$$

where $K_{1,2}$ are the characteristic time constants for processes that lead to changes in the resistance and capacitance, respectively. Assuming that prior to the initiation of breakdown at time t_0, the voltage $V(t)$ and current $I(t)$ are both roughly at a steady state (as corroborated by the curve of Fig. 8 just before 1.15×10^{-7} s), one can obtain the temporal evolution of the circuit current ($I(t>t_0)$ from Eqs. (3) and (4). This leads to the following expression for $I(t)$ valid for times close to t_0:

$$I(t)\sim V(t_0)[-K_2(C_{\text{ini}}-C_f)*\exp(-K_2^*t)+\{(R_{\text{ini}}-R_f)*\exp(-K_1^*t)+R_f\}^{-1}]. \tag{5}$$

In Eq. (5), the voltage at times close to t_0 has been assumed to be nearly constant at $V(t_0)$ Though the above will deviate from the above for longer times, the crude model serves to demonstrate that the presence of the first term on the right-hand side of Eq. (5) can produce a net negative current. Physically, the formation and/or growth of a bubble (or low-density region), leads to the collapse of the local capacitance. Consequently, the stored energy in the capacitor has to be released, and this process serves as a local source of energy that can drive a current. From an electrical circuit standpoint, the release of capacitive energy is akin to the introduction of a local active battery. The precise magnitude of the current evolution is obviously governed by the rate constant K_2, which controls the speed of capacitive collapse. Hence, conceivably if K_2 were large, then the currents, at least at short times immediately following the breakdown initiation, could be negative. At later times, this trend would be overcome by decreases in the resistance, and by changes in the voltage across an elemental unit.

IV. SUMMARY AND CONCLUSIONS

There is considerable interest in the study of electrical breakdown in water (and other liquids) for a variety of applications. These include water-filled gaps for acoustic equipment, the insulation of high-voltage devices, as the medium in spark erosion machines, and as energy storage elements for pulsed power systems. However, the dielectric breakdown phenomenon in liquids is not very well understood, and the development of physical models to simulate the processes remains a germane issue. The breakdown is usually characterized by the occurrence of narrow discharge channels, and a tendency for these channels to branch into complicated stochastic patterns. Hence, any attempts to develop a physically based model needs to include, at the very least, this stochastic element.

Here, a percolative approach to modeling dielectric breakdown has been presented. Conduction is treated in terms of current flows through a network of parallel resistor–capacitor elements having random values (very small deviations based on a Gaussian distribution with fixed mean). The method relies on carrying out self-consistent evaluations of the local potentials based on Kirchhoff circuit analysis at each time step starting from a given initial condition. The local current flows through each elemental unit and local heat dissipation can be determined. A set of two breakdown criteria has been used. One relies on a threshold electric field, and the other, on energy dissipation relative to the heat of vaporization. Improvements to the model used here can be achieved by including more complex I–V characteristics of elements (e.g., nonlinear resistances), and details of ''soft thresholds'' for breakdown. By carrying out his time-dependent analysis of a two-dimensional electrical network, the development and propagation of streamers and prebreakdown dynamical evolution have been obtained directly. Breakdown of the overall structure occurs if a failure channel percolates all the way from one electrode to the other. This model simulation also provides streamer shape and characteristics such as streamer velocity, the prebreakdown delay time, and the relationship between breakdown times and applied electric fields for a given geometry. The results agree well with experimental data and reports in literature.

It has been shown here that despite its simplicity, the model can successfully characterize breakdown and its transient behavior in water. The time to breakdown (t_{br}) for a 100 μm water gap has been shown to be strong function of

the applied bias, with a 15–185 ns range. The voltage dependence of t_{br} was seen to roughly exhibit a $[V/V_{threshold}-1]^{-n}$-type behavior, with $n>1$. The simulation results for t_{br} predicted for the 100 μm gap matched experimental data very well. The current amplitudes were also in accord with measurements, and large swings in both the negative and positive directions were obtained. Based on a simple model, it has been shown here that the current is fashioned not only by dynamic changes in local resistance, but that capacitive modifications arising from vaporization and streamer development also affect the transient behavior. Finally, the model also yielded streamer velocities, which were predicted to be time dependent. A slow initial streamer movement, followed by faster velocities, has been predicted. This general trend and the speed magnitudes are in keeping with reports in literature. A broad conclusion that can be drawn with regard to the development of stable water-based switches is that dielectrics should be chosen not on the basis of their critical hold-off electric field alone. Instead, the thermal conductivity and heat of vaporization must also be important material properties under consideration. It also follows that losses within the liquid dielectric (e.g., to acoustic wave generation, light production, shock-wave initiation, etc.) will similarly have an adverse impact on switch performance. The degree of loss will dictate the extent of spatial variability, and hence, adversely affect the hold-off voltage, the ease of streamer formation, and the current swing.

ACKNOWLEDGMENTS

This work was sponsored by an AFOSR-MURI grant on Compact, Portable Pulsed Power. Useful discussions with S. Katsuki (Kumamoto University) and Edl Schamiloglu (University of New Mexico) are gratefully acknowledged.

[1] H. Akiyama, IEEE Trans. Dielectr. Electr. Insul. **7**, 646 (2000).
[2] J. Talati, T. Shah, A. Memon, M. Sidhwa, S. Adil, and A. Omair, J. Urol. (Baltimore) **146**, 1482 (1991).
[3] A. H. Olson and S. P. Sutton, J. Quant. Spectrosc. Radiat. Transf. **94**, 2226 (1993).
[4] M. Zahn, Y. Ohki, D. B. Fenneman, R. J. Gripshover, and V. Gehman, Jr., Proc. IEEE **74**, 1182 (1986).
[5] M. R. Patel, M. A. Barrufet, P. T. Eubank, and D. D. DiBitonto, J. Appl. Phys. **66**, 4104 (1989).
[6] J. M. Meek and J. D. Craggs, *Electrical Breakdown of Gases* (Wiley, New York, 1978).
[7] E. Nasser, *Fundamentals of Gaseous Ionization and Plasma Electronics* (Wiley, New York, 1971).
[8] R. A. Fava, *Treatise on Material Science and Technology* (Academic, New York, 1977), Vol. 10, Part B, pp. 677–695.
[9] A. Beroual, C. Marteau, and R. Tobazeon, IEEE Trans. Dielectr. Electr. Insul. **23**, 955 (1988).
[10] A. Beroual, J. Appl. Phys. **73**, 4528 (1993).
[11] A. Larsson, A. Sunesson, J. Garmer, and S. Kroll, IEEE Trans. Dielectr. Electr. Insul. **8**, 212 (2001).
[12] R. E. Hebner, J. Phys. D **35**, 205 (2002).
[13] E. O. Forster, IEEE Trans. Dielectr. Electr. Insul. **20**, 891 (1985).
[14] T. J. Lewis, IEEE Trans. Dielectr. Electr. Insul. **20**, 123 (1985).
[15] P. K. Watson, W. G. Chadband, and W. Y. Mak, IEEE Trans. Dielectr. Electr. Insul. **20**, 275 (1985).
[16] P. P. Wong and E. O. Forster, IEEE Trans. Dielectr. Electr. Insul. **17**, 203 (1982).
[17] I. V. Lisitsyn, H. Nomiyama, S. Katsuki, and H. Akiyama, IEEE Trans. Dielectr. Electr. Insul. **6**, 351 (1999).
[18] P. K. Watson and A. H. Sharbaugh, J. Electrochem. Soc. **107**, 516 (1960).
[19] J. V. Coe, A. D. Earhart, M. H. Cohen, G. J. Hoffman, H. W. Sarkas, and K. H. Bowen, J. Chem. Phys. **107**, 6023 (1997).
[20] H. M. Jones and E. E. Kunhardt, J. Appl. Phys. **77**, 795 (1995); H. M. Jones and E.E. Kunhardt, IEEE Trans. Dielectr. Electr. Insul. **1**, 1016 (1994).
[21] L. Gao, A. Larsson, V. Cooray, and V. Scuka, IEEE Trans. Dielectr. Electr. Insul. **6**, 35 (1999).
[22] P. E. Frayssines, N. Bonifaci, A. Denat, and O. Lesaint, J. Phys. D **35**, 369 (2002).
[23] N. Y. Babaeva and G. V. Naidis, J. Phys. D **35**, 132 (2002).
[24] A. Beroual, M. Zahn, A. Badent, K. Kist, A. J. Schwabe, H. Yamashita, K. Yamazawa, M. Danikas, W. G. Chadband, and Y. Torshin, IEEE Electr. Insul. Mag. (USA) **14**, 6 (1998).
[25] O. Lesaint and M. Jung, J. Phys. D **33**, 1360 (2000).
[26] N. Y. Babaeva and G. V. Naidis, J. Phys. D **29**, 2423 (1996).
[27] L. Niemeyer, L. Pietronero, and H. J. Wiesmann, Phys. Rev. Lett. **52**, 1033 (1984).
[28] H. Takayasu, Phys. Rev. Lett. **54**, 1099 (1984).
[29] J. Qian, R. P. Joshi, K. H. Schoenbach, M. Laroussi, E. Schamiloglu, and C. Christodoulou, IEEE Trans. Dielect. Electr. Insul. (to be published).
[30] M. Bartkowiak and G. D. Mahan, Phys. Rev. B **51**, 10825 (1995).
[31] P. M. Duxbury, P. D. Beale, and P. L. Leath, Phys. Rev. Lett. **57**, 1052 (1986).
[32] T. Aka-Ngnui and A. Beroual, J. Phys. D **34**, 794 (2001), and references therein.
[33] T. J. Gallagher, *Simple Dielectric Liquid: Mobility, Conduction and Breakdown* (Oxford University Press, Oxford, 1975).
[34] M. Szklarczyk, in *Modern Aspects of Electrochemistry*, edited by J. O'M. Bockris, B. E. Conway, and R. E. White (Plenum, New York, 1993), Vol. 25, pp. 253–296.
[35] N. J. Felici, IEEE Trans. Dielectr. Electr. Insul. **20**, 233 (1985).
[36] M. Szklarczyk, R. C. Kainthla, and J. O'M Bockris, J. Electrochem. Soc. **136**, 2512 (1989).
[37] L. Onsager, J. Chem. Phys. **2**, 599 (1934).
[38] F. Pontiga and A. Castellanos, IEEE Trans. Dielectr. Electr. Insul. **3**, 792 (1996).
[39] T. S. Light, Anal. Chem. **56**, 1138 (1984); T. S. Light and S. L. Licht, *ibid.* **59**, 2327 (1987).
[40] D. B. Fenneman and R. J. Gripshover, IEEE Trans. Plasma Sci. **8**, 209 (1980).
[41] S. Katsuki, R. P. Joshi, M. Laroussi, and K. H. Schoenbach, "Electrical and Optical Characteristics of Water under High Electric Stress," Proceedings of the 25th IEEE Power Modulators Conference, Hollywood, CA, June 30–July 3, 2002; K. H. Schoenbach, S. Katsuki, S. Xiao, F. Leipold, M. Laroussi, R. P. Joshi, and J. B. Cooper, "Electrical Breakdown of Submillimeter Water Gaps," Proceedings of the International Conference on High Power Particle Beams, Albuquerque, NM, June 23–28, 2002.